

# Total Synthesis and Retrosynthesis Study of Astellolide R

Baoyi Chen<sup>1,a,†</sup>, Ling Hao<sup>2,b,†,\*</sup>

<sup>1</sup>International School on the Rhine, Neuss, 41464, Germany

<sup>2</sup>Shenzhen MSU-BIT University, Shenzhen, 518172, China

<sup>a</sup>bonniechen0909@gmail.com, <sup>b</sup>935196618@qq.com

\*Corresponding author

†All the authors contributed equally to this work and should be considered as co-first

**Abstract:** Astellolide R, a juniperane-type sesquiterpenoid with the molecular formula  $C_{15}H_{18}O_4$ , is a rare and structurally intricate natural product especially distinguished by its cage-like pentacyclic structure, dioxabicycloheptane moiety, multiple ether linkages, and five carbon stereocenters. These highly unusual features contribute to both its distinctive reactivity and potential biological significance, while posing formidable challenges for synthetic access. Another factor that makes the access as well as studies in this area more challenging is due to Astellolide R being previously discovered not so long ago. In this study, we conducted a retrosynthetic and synthetic analysis of three distinct pathways aimed at constructing and reconstructing the Astellolide R scaffold, and each of the pathways offer unique approaches and results, such as using Zirconocene paired with photocatalysis, and getting commercially available products like Drimendiol.

**Keywords:** Astellolide R, Sesquiterpenoid, Zirconocene, Drimendiol, Photocatalysis

## 1. Introduction

### 1.1 Astellolide R Overview

An important factor for discovering new drugs and developing drugs are natural products, because they almost always offer diverse structures and they mostly have unique biological activity that will assist in making advancements in new therapeutics. Among all of these natural products, sesquiterpenoids, which are compounds that consist of three isoprene units, and a class of terpenes are rich in secondary metabolites, and they are known for their complicated structures and a diverse range of properties. Astellolide R, which is a sesquiterpenoid, was recently identified. It is a juniperane-type sesquiterpenoid with a molecular formula of  $C_{15}H_{18}O_4$ , and it is an example of when a structure is complex and consists of natural products. Its structure is distinguished by a cage-like pentacyclic framework and a rare dioxabicycloheptane moiety, along with its five stereocenters and multiple ether linkages that contribute to both the unique 3D shape of Astellolide R and its reactivity. These features of Astellolide R are not usually seen combined, and it makes this molecule an interesting synthetic and retrosynthetic target [1].

### 1.2 Approach for the total synthesis and retrosynthesis of Astellolide R

The total synthesis of Astellolide R and natural products are generally not explored as much as the other polycyclic sesquiterpenoids even though there is an increasing interest in this field. The exploration of Astellolide R as an example is challenging because it has a rigid framework and there is a high difficulty of selectively cleaving each ether linkage, and reforming them within the polycyclic frameworks. The common and most conventional synthetic approaches would often require more complicated sequences, harsh, strong reaction conditions and expensive catalysts to carry out, which will have an impact and limit their percentage yield and efficiency. At the same time, another method could be used which is derived from the recent advancements in selective bond activity, photoredox catalysis and the use of precursors which are available naturally. This method will expand the options available for pushing past these challenges, and we will be using these ways for our approach to do the total synthesis and retrosynthesis of Astellolide R.

### 1.3 Total synthesis Analysis

Because of this, we felt ambitious and we were aspired to evaluate the potential synthetic strategies that we can use through analysis synthetically and retrosynthetically. Our aim was to identify potential disconnections and transformations that are feasible, and potentially improve the speed of access to Astellolide R and open new approaches to other complex molecules of this type. To achieve a feasible synthesis, we created three pathways with one main and two alternatives: a modernised Zirconocene photocatalysis approach for selective ether cleavage within the Drimane framework molecule, another route, which is a simple route leveraging drimendiol as a commercially available starting material, and lastly a literature supported but more demanding sequence in terms of money, availability and it also involves oxidative rearrangements and rhodium catalysed couplings.

## 2. Approach

### 2.1 Summary of Primary Research

#### 2.1.1 Introduction to our research

Our synthetic and retrosynthetic analysis starts with identifying the most important functional groups within the target molecule throughout, with emphasis mainly on the conformational constraints and the challenges that are thrown upon us by its cage-like framework and how we will construct and deconstruct it. This feature of Astellolide R limits the applicability of conventional function group transformations, thus necessitating highly selective bond-cleavage strategies.

#### 2.1.2 Where inspiration comes from

In developing the retrosynthetic strategy, we drew inspiration from the concept of Asymmetric Diversity Oriented Synthesis (aDOS). We envisioned starting from the two ether bridges of Astellolide R, and through stepwise ether bond cleavage, dismantling the 3D cage-like structure into a more planar cyclic intermediate framework, which could then be traced back to more accessible precursor fragments.

## 2.2 Synthetic Pathway Step Analysis

### 2.2.1 Photoredox cleavage of the C13–O–C15 bond

To achieve this goal, we selected a system of photoredox catalysis combined with Zirconocene catalysis, which can effectively cleave C–O bonds in epoxide-like structures, while DDQ-induced oxidative cleavage is suitable for further ether bridge opening, converting them into hydroxyl and methyl functionalities.

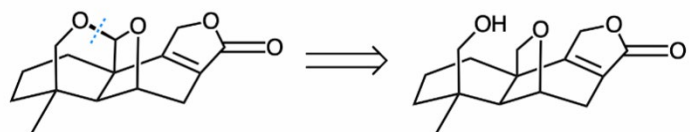


Figure 1 Selective Cleavage of C13–O–C15

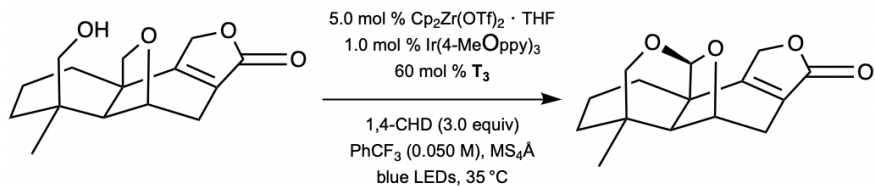


Figure 2 Synthetic Reaction to Make Astellolide R

The two key ether bonds of Astellolide R are C13–O–C15 and C15–O–C6. In our retrosynthetic analysis, shown in Figure 1, we first envisioned selective cleavage of the C13–O–C15 ether bond to weaken the conformational restrictions of the cage-like framework and obtain a more planar skeleton.

The preference for this cleavage pathway is based on combined structural electronic and steric considerations: C15, as a bridgehead carbon located at the junction of the tricyclic system, bears significant bond strain and steric hindrance. In the C13–O–C15 bond, C13 is a primary carbon located at the peripheral methylene bridge, making it more sterically accessible. In this position, the radical that is generated here can prove useful reactivity in the next steps of the reaction. On the other hand, the C6 is located much deeper inside the framework of the molecule, and it is part of the six-membered ring formed with C5 and C7, and this framework is the main framework of the molecule, where the atoms surrounding it create stronger steric shielding effects. Because of this environment, C6 is less likely to interact with the catalyst effectively, as bonds are less likely to be broken here or cleaved off.

The strategy in Figure 2 that we used takes inspiration from literature [2], which describes the use of a photoredox-Zirconocene catalytic system that works under milder conditions, which uses blue light irradiation ( $\lambda = 450$  nm) at room temperature to selectively break the strained ether bonds. We know that the polycyclic framework of Astellolide R is complex and there is a steric hindrance around the C13–O–C15 ether bond, we considered the approach in literature [2] strong and relevant. In the literature, it demonstrated that  $\text{MeOppy}_3$  (P1) exhibited higher catalytic efficiency and broader substrate scope compared to  $[\text{Ir}\{\text{dF}(\text{CF}_3)\text{ppy}\}_2(\text{dtbbpy})]\text{PF}_6$  (P3) in such systems. Therefore, P1 was chosen as the photocatalyst for this specific bond cleavage, with 1,4-cyclohexadiene used as a hydrogen donor. Importantly, this catalytic system is not only effective at activating the epoxides and ethers at the bridgehead, but also it illustrates strong tolerance for polycyclic structures like Astellolide R that are complicated, which is important for our case as that is our target molecule.

Based on the literature and our findings, we proposed to apply this method by applying this photocatalytic system to cleave the C13–O–C15 ether bond in Astellolide R. Doing this bond cleavage is expected to yield an intermediate that contains a hydroxyl group at C13 while still preserving the bridge, which is important as it is selective. This transformation can potentially relieve the ring strain internally, and thus making the overall molecule framework flatter, to open up new opportunities for simplification of complex skeletons. In addition, to prevent mixed or partial cleavage, the exact cleavage site can be pinpointed through careful analysis using  $^1\text{H}$  NMR together with HSQC and HMBC experiments.

### 2.2.2 DDQ oxidation of the C15–O–C6 bond

After completing C13–O–C15 bond cleavage to yield the partially planarized intermediate, we further propose selective cleavage of the C15–O–C6 ether bond to completely open the cage like framework of Astellolide R. To this end, we adopt the widely applied DDQ mediated oxidative cleavage strategy [3]. This method can selectively cleave ethers under mild conditions, especially suited for bridging ethers with high stability, while exhibiting good functional group compatibility and regioselectivity. Literatures show that addition of DDQ to the substrate in THF at  $-78^\circ\text{C}$  followed by warming to room temperature achieves efficient oxidative ether cleavage.

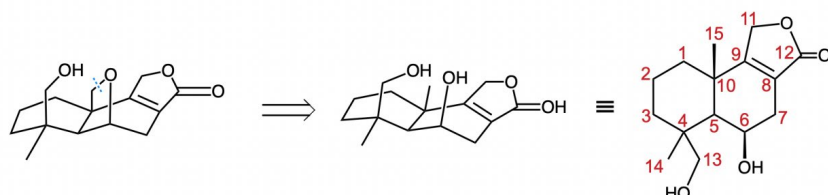


Figure 3 Generating A Hydroxyl Group At C6, And Oxidation At C15

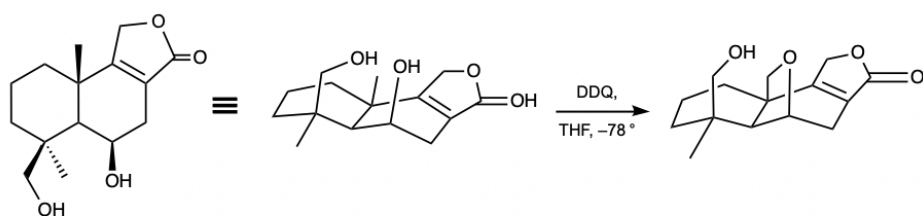


Figure 4 Reconstructing the Cage-Like Framework

By applying this approach to the C15–O–C6 bond shown in Figure 3, Astellolide R would yield a hydroxyl group at C6, while oxidation at C15 would generate a methyl group. This change would

completely break apart the cage-like framework, increase planarity, and make the structure better suited to aDOS requirements for open precursor frameworks. The practicality of this tactic is supported by precedent in oxidative ether cleavage steps from natural product synthesis, offering a solid theoretical foundation for its inclusion as a key step in retrosynthetic planning. In the synthesis step in demonstrated in Figure 4, the cage-like framework is reconstructed.

### 2.2.3 Ozonolysis and reduction to make key intermediate

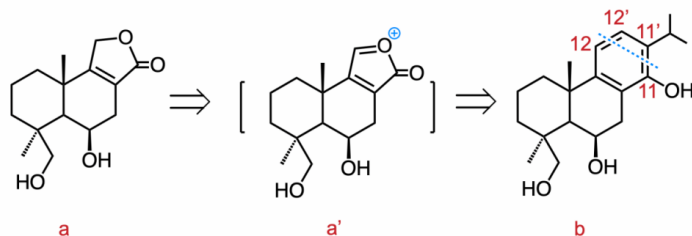


Figure 5 One-Pot Ozonolysis Reduction

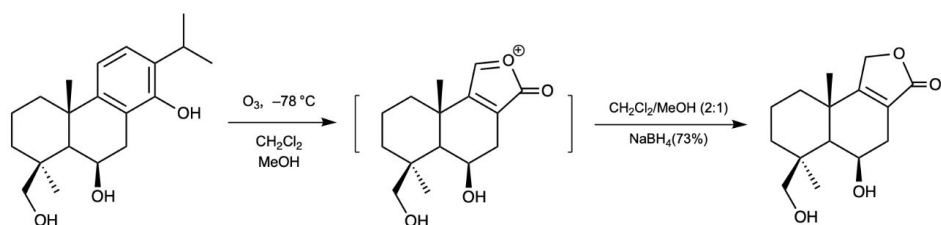


Figure 6 Synthesis Of A

With the double ether cleaved intermediate available, we continued backtracking the structure, primarily focusing on the core lactone ring. In Figure 5 we utilized literature strategies for constructing lactones from phenols proposing a reverse pathway from  $a \rightarrow a' \rightarrow b$ . In the reference this step was achieved through a one-pot ozonolysis-reduction sequence: at  $-78^{\circ}\text{C}$  and ozone was bubbled through a  $\text{CH}_2\text{Cl}_2/\text{MeOH}$  (2:1) solution followed by  $\text{NaBH}_4$  reduction. This effected double oxidative cleavage of the  $\text{C}11/\text{C}11'$  and  $\text{C}12/\text{C}12'$  carbon-carbon (C-C) bonds on the phenol ring, forming oxonium ion intermediate  $a'$ , which was subsequently reduced to lactone  $a$  in 73% yield. [4]

From a retrosynthetic perspective, portrayed in Figure 6, this represents a crucial ring cleaving step because this allows us to envision the lactone framework all the way back from phenol  $b$  by double ozonolysis and reduction. The strategy that we used can have a great value in natural product synthesis, because it provides a reliable way to selectively dismantle the sterically hindered units in especially complex systems like Astellolide R, and this approach offers good retrosynthetic utility.

### 2.2.4 Building the lactone ring and flattening the framework

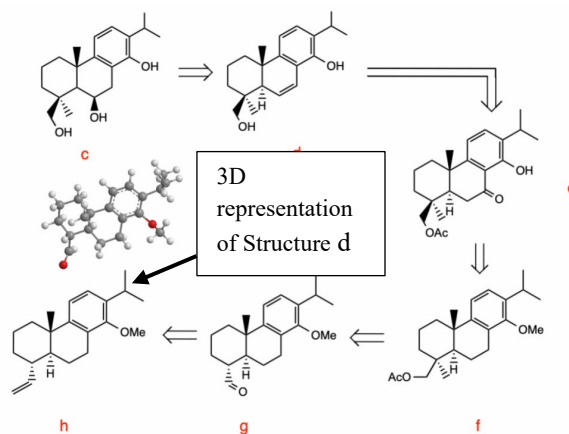
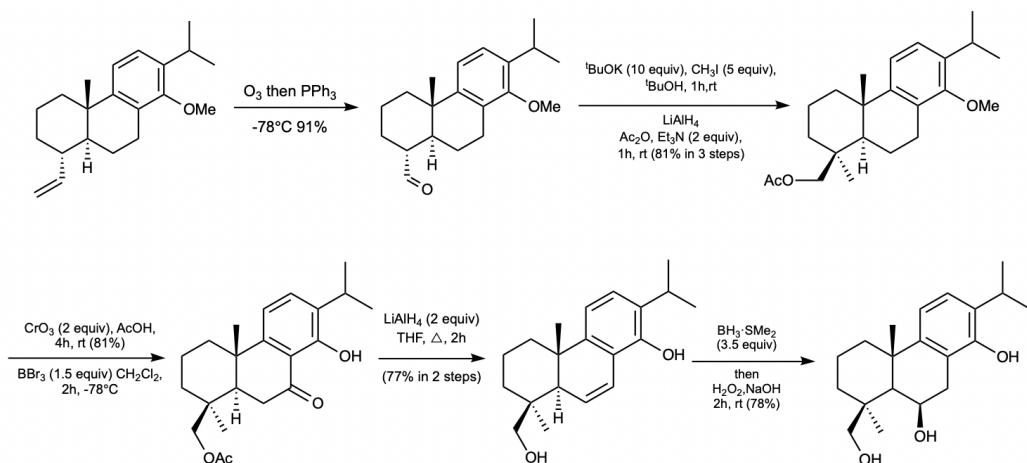


Figure 7 Aldehyde Alkylation, Reduction, Oxidation And Reductive Sequences

Figure 8 Synthesis Of *c* By Given Conditions

Further retrosynthetic analysis of phenol *l* follows the literature route in which it is derived from the drimane-type tricyclic skeleton *h*, indicated in Figure 7. The sequence proceeds through stepwise functionalization of the carbon framework. The sequence includes: Aldehyde alkylation, followed by reduction then oxidation, and lastly reductive transformations, concluding in installation of the hydroxyl and aromatic features characteristic of phenol *c*.

In detail, aldehyde *g* is enolized with  $\text{t-BuOK}$  and alkylated with  $\text{MeI}$  to give an alkylated intermediate, which is then reduced with  $\text{LiAlH}_4$  and acetylated under  $\text{Ac}_2\text{O}/\text{Et}_3\text{N}/\text{DMAP}$  conditions to furnish *f* in 81% overall yield over three steps [5]. A critical aspect here is the construction of the tetrasubstituted stereocenter at C4; as noted in the literature, conformational bias directs methylation from the less hindered face providing high stereoselectivity.

Compound *f* in Figure 7 is next oxidized with  $\text{CrO}_3$  to the corresponding ketone, followed by demethylation to afford aryl ketone *e*. Reduction of *e* with  $\text{LiAlH}_4$  initiates a reductive cascade to produce *d*. Subsequent reduction with  $\text{BH}_3 \cdot \text{SMe}_2$  and oxidation with  $\text{H}_2\text{O}_2$  selectively installs a hydroxyl group at C6, delivering the target phenol *c* in 78% yield.

This approach combines precise stereo control with efficient functional group manipulation, offering a robust and literature-supported pathway. In our retrosynthetic plan, we adopt this strategy to progressively simplify the tricyclic skeleton while increasing planarity, using highly selective aldehyde-based transformations to enable controlled, stepwise dismantling. Figure 8 shows the synthesis of *c* in that is present in Figure 7 by the given conditions.

### 2.2.5 Aldehyde alkylation and redox sequence

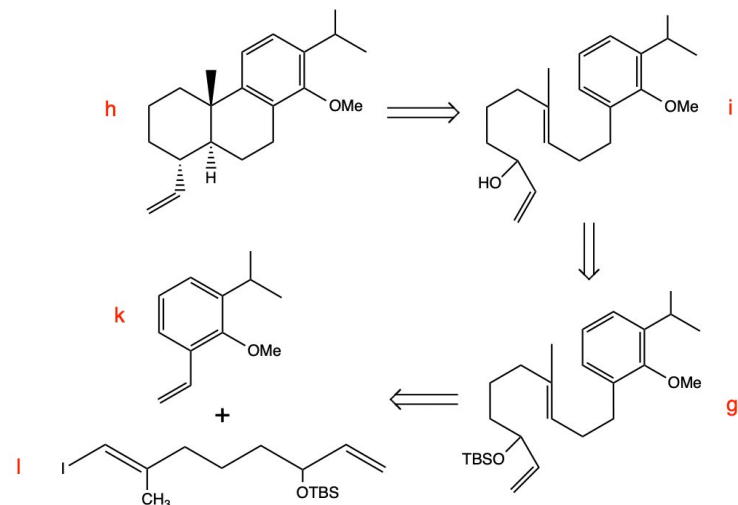


Figure 9 Lewis Acid Catalyzed Polyene Cyclization

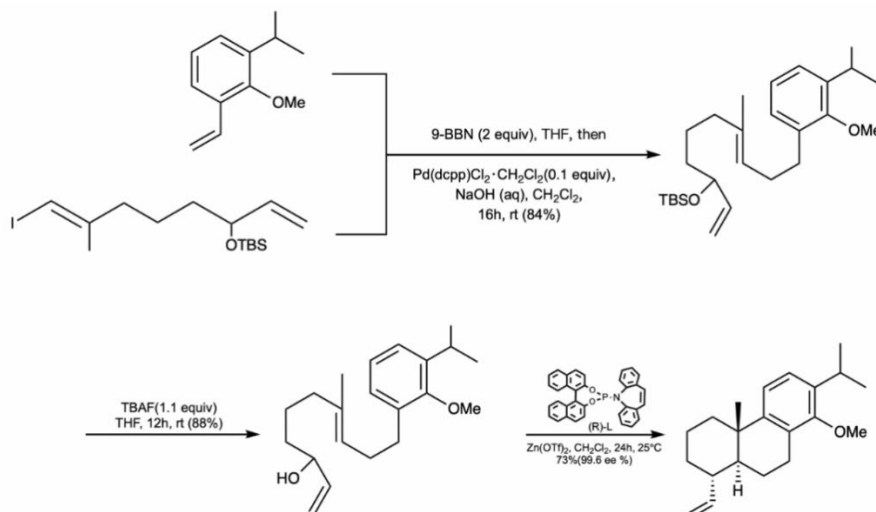


Figure 10 Synthesis of H from Suzuki Coupling of K And L

To further depict the building the tricyclic skeleton, we examined the synthesis of drimane skeleton h. Literature reports an asymmetric Lewis acid-catalyzed polyene cyclization using Zn(OTf)<sub>2</sub> (20 mol%), giving drimane skeleton h in 73% yield and 99.6% ee. This reaction represents the stereocontrolling key step of the total synthesis [6].

Polyene i, the cyclization substrate in Figure 9, was obtained from intermediate g by deprotection of a silyl ether using TBAF (tetrabutylammonium fluoride) under mild conditions with good functional group tolerance. Intermediate g itself was prepared by treating styrene derivative k with 9-BBN to form a boron reagent, followed by Suzuki coupling with vinyl iodide l using Pd(dppf)Cl<sub>2</sub>·CH<sub>2</sub>Cl<sub>2</sub> and NaOH. The two step overall yield was 74%. [6] In this construction strategy, the silyl ether protection was intentionally retained through the coupling step to improve functional group compatibility and provide conformational preorganization for the subsequent polyene cyclization.

Therefore, in Figure 9, starting from intermediate a, we trace back stepwise to the polyene substrate i that constructs the tricyclic core, and further back to the Suzuki coupling intermediates k and l, forming a highly possible and continuous synthetic pathway, which is Figure 10, formed by the synthesis of h and the Suzuki Coupling of k and l, also backed up by the retrosynthetic pathway.

#### 2.2.6 Polyene cyclization to form tricyclic skeleton

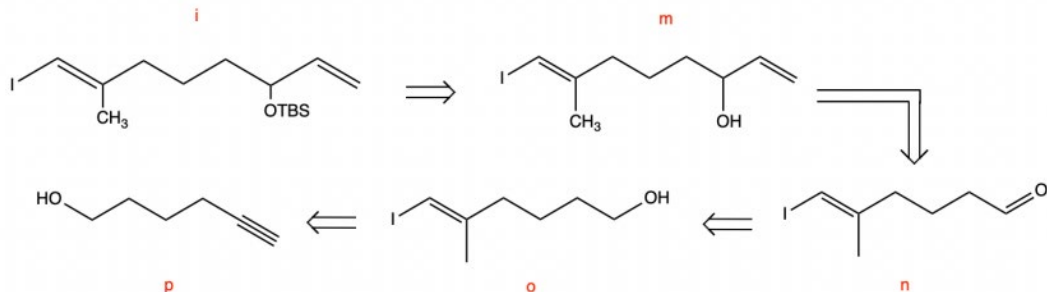


Figure 11 Back-Tracking of Vinyl Iodide to Precursor Compounds

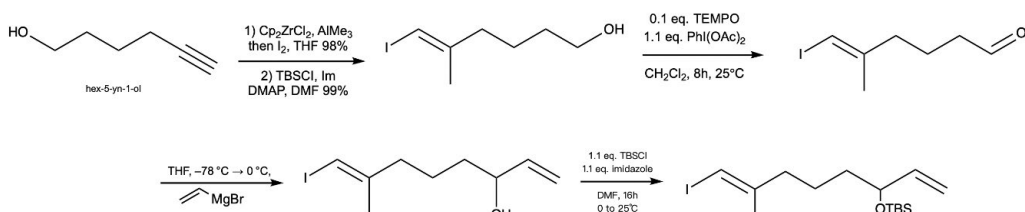


Figure 12 Synthesis of I

To continue the construction pathway of vinyl iodide *i*, we analyzed the synthetic strategy for this key intermediate. According to the route proposed in [7], vinyl iodide *i* was prepared from a hydroxyl containing alkyne compound through a series of carefully designed transformations. In the retrosynthetic analysis, we back-tracked from vinyl iodide *i* to its precursor compounds, ultimately arriving at hydroxyl-containing alkyne *p* as a relatively simple starting material.

Figure 11 involves four key transformations. First, hydroxyl containing alkyne *p* was converted into an iodinated alcohol following the method described in reference [7]. The reaction contained  $\text{Cp}_2\text{ZrCl}_2$  and  $\text{AlMe}_3$  followed by the addition of  $\text{I}_2$  in THF. Astonishingly, the product produced is up to 98% yield. This transformation converted the alkyne moiety into an iodo-enol laying the foundation for the subsequent steps. Next, the iodinated alcohol went through selective oxidation with 1.1 equivalents of  $\text{PhI}(\text{OAc})_2$  and 0.1 equivalents of TEMPO in dichloromethane ( $\text{CH}_2\text{Cl}_2$ ) at room temperature ( $25^\circ\text{C}$ ) for 8 hours ultimately making aldehyde-containing compound *n*. This TEMPO-catalyzed oxidation selectively transformed the primary alcohol into an aldehyde generating an appropriate electrophile for the upcoming C–C bond forming reaction.

In the third step, compound *n* reacted with vinylmagnesium bromide in THF at  $-78^\circ\text{C}$  to  $0^\circ\text{C}$  for 1 hour to give hydroxyl-containing compound *m*. Conducting the Grignard reaction at low temperature effectively controlled selectivity and yield which allowed this reaction to successfully introduce the vinyl fragment. Finally compound *m* was treated with 1.1 equivalents of  $\text{TBSCl}$  (tert-butyldimethylsilyl chloride) and 1.1 equivalents of imidazole in DMF at  $0\text{--}25^\circ\text{C}$  for 16 hours, affording the desired vinyl iodide *i* as its OTBS-protected derivative in 84% yield. This silyl protection reaction performed under mild basic conditions, which effectively protected the hydroxyl group and provided a stable substrate for next coupling reactions.

In summary, the pathway proposed of vinyl iodide *i* reveals the transformations made each step in a sequence from the target molecule back to the simple starting alkyne. This route incorporates protecting the groups chemistry, redox reactions/transformations, C–C bond formation and functional group conversions internally. Each of the steps directly corresponds to a forward synthetic transformation, with reaction conditions, mechanisms, and yields that are considered with further thought in the overall design. Although the hydroxyl-containing alkyne is not by itself a final commercial raw material (a material that can be bought on the market), this analysis shows an in depth foundation for the development of more efficient and possibly economically viable synthetic route (Figure 12) that can be utilized in the future.

### 2.2.7 Retrosynthetic route to the starting material

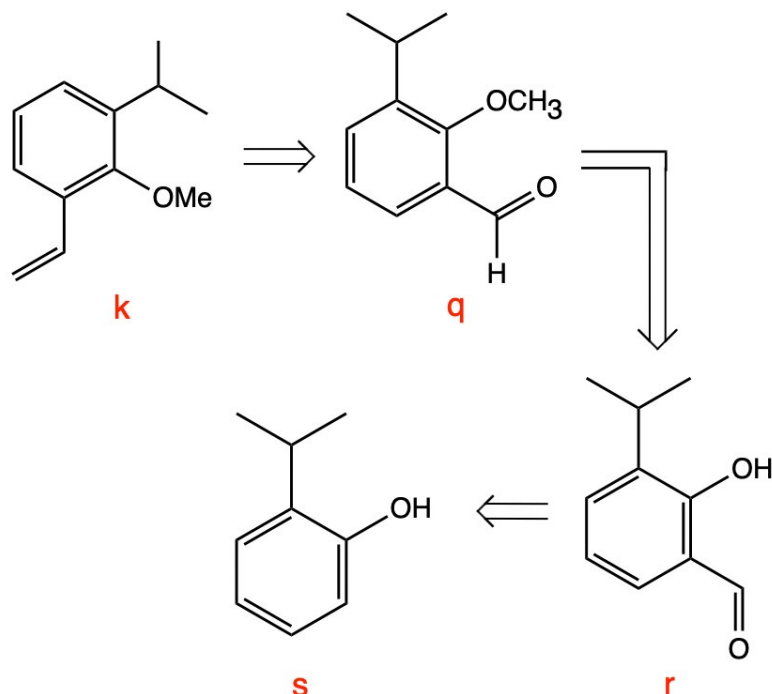


Figure 13 3 Step Reaction to Get Product *S*

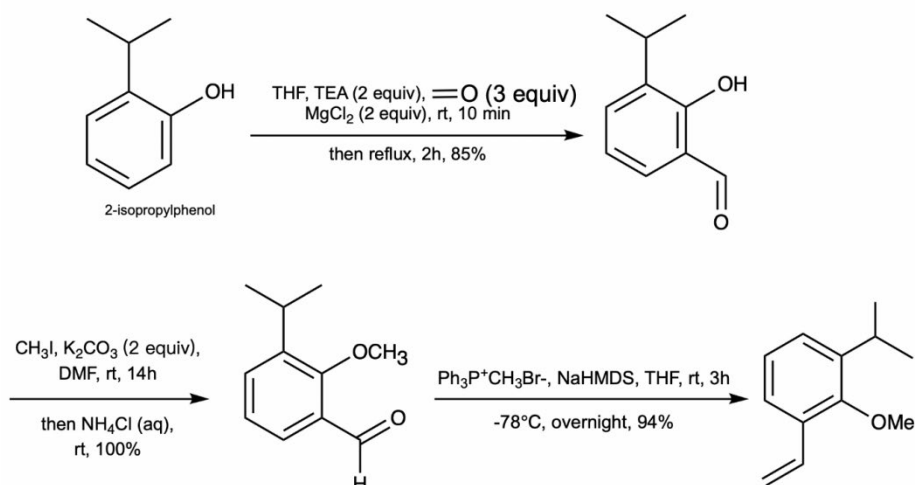


Figure 14 Synthesis Reaction To Give Substituted Styrene K

First, in Figure 13, 2-methoxy-3-isopropylbenzaldehyde *q* reacts with methyltriphenylphosphonium bromide ( $\text{Ph}_3\text{P}^+\text{CH}_3\text{Br}^-$ ) in the presence of a strong base (such as sodium bis(trimethylsilyl)amide, NaHMDS) in tetrahydrofuran (THF) at room temperature for 3 hours, followed by stirring overnight at  $-78^\circ\text{C}$ , to give substituted styrene *k* in 94% yield. This is a classic Wittig reaction, in which a phosphonium ylide reacts with an aldehyde to efficiently construct a carbon–carbon double bond, introducing a vinyl group. This reaction, as described in reference [8], serves to convert the aldehyde into an olefin, thus preparing it for subsequent coupling with the aromatic ring.

Next, phenol *r* undergoes an alkylation reaction with a bromide in the presence of potassium carbonate ( $\text{K}_2\text{CO}_3$ ) in DMF, followed by aqueous work-up with ammonium chloride ( $\text{NH}_4\text{Cl}$ ) solution, affording the corresponding methoxy-substituted benzaldehyde derivative *q* in quantitative (100%) yield. The key point of this step is the introduction of a specific substituent via alkylation, thereby efficiently building the intermediate structure necessary for the next stage of synthesis.

Finally, phenol *s* reacts with formic acid in the presence of triethylamine and magnesium chloride in THF, stirred at room temperature for 10 minutes and then heated to reflux for 2 hours, giving the derivative (with a lactone structure) in 85% yield. This step converts the phenol into a substituted salicylaldehyde derivative bearing an aldehyde group, which is then used for the synthesis of a chromium catalyst ligand.

In summary, the pathway for substituted styrene *k* reveals a clear step-by-step transformation from the target molecule back to simple starting materials. The route incorporates the Wittig reaction, methyl ether formation, and construction of the benzaldehyde framework. Each retrosynthetic step corresponds closely to the reaction conditions, mechanisms, and yields in the forward synthesis, and their feasibility and efficiency must be carefully considered when designing the synthetic scheme. Although benzaldehyde and 2-isopropylphenol are relatively simple commercial starting materials, this in-depth analysis at this stage lays a solid foundation for a more efficient and cost-effective synthetic route, which is Figure 14, showing the following synthesis reaction that can take place to produce the substituted Styrene *k*.

### 3. Discussion - Significance of Pathway

Both the retrosynthetic and synthetic analysis of Astellolide R shows the challenges and as well as the potential opportunities that it might give in a next new step towards synthesizing complex natural products. Its cage-like pentacyclic framework structure has multiple ether linkages and stereocenters, making places where there will be constraints that will influence the reactivity and additionally will also affect the biological interactions. These elements of the unique structure will then further complicate the synthetic planning while also showing how much potential the compound has and how it might become more biologically relevant now, making Astellolide R a great target to work towards development of drugs, even if it has weak inflammatory properties.

In this research paper, we compared between the three routes that we proposed, and this reveals the clear differences between the efficiency, selectivity and how innovative each route is. Pathway 1 relies

on a stereocontrolled strategy that gets the stereochemistry that is desired with lots of precision, however there are many strict reaction conditions required in order to complete this pathway. Pathway 2 uses a fragment-based assembly that allows a good amount of flexibility in the designing process, however the practicality of this path was reduced because of its lower bond selectivity and byproduct formation. Lastly, pathway 3 introduced a catalytic transformation for complex ether bond formation, which offers a forward-looking approach. However, the methods used are relatively new and unconventional, so it created new challenges to consider such as how feasible it is to be reproduced. From this discussion, we learn that the efficiency, innovation and selectivity are all important in modern designs of synthesis. Efficiency involves reducing the step count and maximizing the yield. Innovation offers ways to overcome the barriers, as it will use other emerging methods and selectivity ensures that the correct stereochemistry is obtained for the best biological activity.

Not considering just the synthetic aspect, our studies hold further and broader ideas for potential pharmaceutical research. Because Astellolide R belongs to the juniperane-type sesquiterpenoids which is known for its unique biological activity, developing reliable synthetic pathways not only will open up and prepare the natural product itself but this also supports the creation of structural counterparts. These counterparts could accelerate the discovery of more derivatives with enhanced and more effective pharmacological properties.

Finally, to wrap up, by applying the green chemistry principles it reveals that there is a limitation in this study. The limitation is that it needs better atom economy and considerations in the sustainability in complex molecule synthesis and retrosynthesis. While each of the pathways that we proposed showed unique strengths, in the future we should further consider and address environmental and industrial factors by researching and using more sustainable catalysts, more environmentally friendly solvents in the reactions, and possibly biocatalytic processes.

#### 4. Conclusion

Finally, to conclude our research, we think that the total synthetic and retrosynthetic analysis and exploration of the molecule Astellolide R adds onto the studies in structurally complex natural products by balancing efficiency, selectivity and creativity. Astellolide R's cage-like pentacyclic framework, ether linkages and the five stereocenters presented significant challenges for us but it also offers a lot of opportunities for advancement in the field of complex molecules and sesquiterpenoids. The comparison that we did between these three pathways, both distinctive in their own ways show the differences between the cost and availability of resources that are used, for instance, catalysts. Beyond the synthetic strategies, this provides a new area for exploring the structure and activity in relation of each other and creating derivatives with better potential to be employed for pharmaceutical uses. Future improves can be integrating green chemistry principles and applying the advanced modern design and this will help improve the atom economy and sustainability. These optimizations will be important for expanding the scope of complex molecule synthesis and enabling its use in drug development.

#### References

- [1] Dai, G.; Sun, J.; Peng, X.; Shen, Q.; Wu, C.; Sun, Z.; Sui, H.; Ren, X.; Zhang, Y.; Bian, X. *Astellolides R-W, Drimane-Type Sesquiterpenoids from an Aspergillus parasiticus Strain Associated with an Isopod*. *J. Nat. Prod.* 2023, 86, 1746–1753. <https://doi.org/10.1021/acs.jnatprod.3c00215>.
- [2] Aida, K.; Hirao, M.; Fundabashi, A.; Sugimura, N.; Ota, E.; Yamaguchi, J. *Catalytic Reductive Ring Opening of Epoxides Enabled by Zirconocene and Photoredox Catalysis*. *Chem* 2022, 8 (6), 1762–1774. <https://doi.org/10.1016/j.chempr.2022.04.010>.
- [3] Qiu, H.; Fei, X.; Yang, J.; Qiao, Z.; Yuan, S.; Zhang, H.; He, L.; Zhang, M. *A Bischler–Napieralski and Homo-Mannich Sequence Enables Diversified Syntheses of Sarpagine Alkaloids and Analogues*. *Nat. Commun.* 2023, 14, 5560. <https://doi.org/10.1038/s41467-023-41268-9>
- [4] Lai, Y.; Zhang, N.; Zhang, Y.; Chen, J.-H.; Yang, Z. *Asymmetric Total Syntheses of Insulicolide A, 14-O-Acetylinsulicolide A, 6β,9a-Dihydroxy-14-p-nitrobenzoylcinnamolide, and 7a,14-Dihydroxy-6β-p-nitrobenzoylconfertifolin*. *Org. Lett.* 2018, 20 (15), 4471–4474. <https://doi.org/10.1021/acs.orglett.8b01733>.
- [5] Schafroth, M. A.; Sarlah, D.; Krautwald, S.; Carreira, E. M. *Iridium-Catalyzed Enantioselective Polyene Cyclization*. *J. Am. Chem. Soc.* 2012, 134 (52), 20276–20278. <https://doi.org/10.1021/ja310386m>
- [6] Thalji, R. K.; Roush, W. R. *Remarkable Phosphine Effect on the Intramolecular Aldol Reactions of*

*Unsaturated 1,5-Diketones: Highly Regioselective Synthesis of Cross-Conjugated Dienones.* *J. Am. Chem. Soc.* 2005, 127 (51), 16840–16851. <https://doi.org/10.1021/ja056548d>.

[7] Sun, M.; Xu, T.; Gao, W.; Liu, Y.; Wu, Q.; Ye, L.; Mu, Y. *Large Ultra-High Molecular Weight Polyethylene Spherical Particles Produced by AlR<sub>3</sub> Activated Half-Sandwich Chromium(III) Catalysts.* *Dalton Trans.* 2011, 40 (39), 10184–10194. <https://doi.org/10.1039/c1dt10659g>.

[8] Goncalves, S.; Santoro, S.; Nicolas, M.; Wagner, A.; Maillos, P.; Himo, F.; Baati, R. *Cationic Cyclization of 2-Alkenyl-1,3-dithiolanes: Diastereoselective Synthesis of trans-Decalins.* *J. Org. Chem.* 2011, 76 (9), 3274–3285. <https://doi.org/10.1021/jo2001116>.